# The Structure of the Nucleon Studied with the Electroweak Probe*

D. Drechsel
Institut *für Kernphysik,* Johannes *Gutenberg-* Uniuersitat
Mainz, *D-55099* Mainz, *Germany*

Received November 10, 1993

Charged leptons are an ideal probe to study the hadronic structure of nucleons. Such investigations become even more interesting in view of the somewhat puzzling results about the spin structure of the nucleon in deep inelastic scattering. The advent of a new generation of high-energy, high-intensity electron accelerators operating with a continous beam opens a new frontier of coincidence experiments with polarization degrees of freedom. Such investigations will provide precise form factors of proton and neutron over a large range of momentum transfer. The parity-violating scattering of polarized electrons is expected to give us first direct informations on the strangeness inside the nucleon and its contribution to the charge and the magnetization distributions. The most recent results in deep inelastic scattering off the neutron indicate that at least the difference of neutron and proton is compatible with the requirements of quantum chromodynamics ('Bjorken sum rule'), but tlie discussion about the carriers of the nucleon's spin is still controversial. Finally, there are certain expectations from perturbative quantum chromodynamics about the quasifree reaction (e, $e'N$) on a heavy nucleus ('colour transparency') which remain to be tested by new experiments.

## I. fntroduction

Since the electromagnetic interaction is governed by the fine structure constant $\alpha = e^2/4n \approx 1/137$, the one-photon exchange approximation (see figure 1) has an accuracy of about 1% for electron scattering off the nucleon and light nuclei. In the case of weak neutral currents (exchange of $\mathcal{Z}^o$ gauge boson) the interaction is even weaker, by orders of magnitude in the low energy regime, such that only its interference terms with the electromagnetic interaction may become visible. The four-momentum of the exchanged photon, $q = (w, \vec{q}) = k_i - k_f$, is fixed by the four-momenta of the incident and outgoing electrons, respectively. In general we will assume that the initial hadronic system is a nucleon, $P^2 = m^2$, where m is the mass of the nucleon. The target nucleon may be polarized, usually with spin parallel or antiparallel to the real or virtual photon, leading to excited states with overall helicity $1/2$ or $3/2$. In the following we will only discuss inclusive scattering, i. e. the final state of the hadronic system will not be resolved. Due to momentum conservation the momentum $P'$ of the hadronic final state is fixed, leaving two independent variables to describe the hadronic vertex. It is customary to define as one of these variables $Q^2 = -q^2$, because this quantity is always positive in the case of electron scattering (virtual photon exchange), while it vanishes for the absorption of a real photon. (Note that negative values are reached by lepton pair annihilation). The second independent scalar is the Mandelstam variable $s = W^2 = (P + q)^2$, related to the total *c.m.* energy W. In the case of elastic scattering, $s = m^2$, leaving only $Q^2$ as a variable. For inelastic processes $s \geq (m + m_\pi)^2$, where $m_\pi$ is the mass of the pion defining the lowest threshold. The relation between energy and momentum transfer for various physical phenomena can be best discussed in terms

*This work was supported by the Deutsche Forschungsgemeinschaft (SFB 201)

of the Bjorken scaling variable

$$x = \frac{Q^2}{2P \cdot q} = \frac{Q^2}{2m\omega_L} = \frac{Q^2}{W^2 - m^2 + Q^2}, \qquad (1)$$

where $\omega_L$ is the energy of the photon in the laboratory frame. The Bjorken variable is unity in the case of elastic scattering on a nucleon and decreases to smaller values with increasing inelasticity (W > m). We note that the value $x = 0$ is obtained for real photons ($Q^2 = 0$) arid also approached for large inelasticities ($W \gg m, Q^2$). Elastic scattering on a nucleus with mass $M = Am$ requires $Q^2 = 2M\omega_L$, and the scaling variable takes the value

$$x = \frac{Q^2}{2m\omega_L} = \frac{M}{m} = A. \qquad (2)$$

Inelastic exc tations of collective type, such as shape oscillations, rotations or giant resonances require the cooperation of many nucleons. In that sense the collective (inelastic) response of a nucleus occurs at $x \leq A$. However, these resonances do not define a fixed relation between energy and momentum transfer. Instead they disappear rapidly with increasing spatial resolution (i. e. momentuin transfer). At the same time we should observe less cooperative phenomena, like clusters involving only a few nucleons. In particular, the nuclear response for $x \leq 2$ should be dominated by short-range correlations between pairs of nucleons ('quasi-deuteron effect').

The region $x \approx 1$ corresponds to scattering on single nucleons ( 'quasi-free scattering'). Slightly below $x = 1$ we expect to see the isobars as 'coherent' excitation modes of quarks in nucleons, exhibiting a dependente on both energy and momentum transfer. However, if both energy and momentum transfer are sufficiently high compared to binding energies and Fermi motion, we observe incoherent and elastic scattering off the constituents (partons) of the nucleon ('deep inelastic scattering' = DIS). In this range the response of the hadronic system can be described, once more, by the scaling variable x only. In the most naive picture of 'constituent quarks' with mass $m_q \approx \frac{1}{3}m$, we expect quasi-free scattering of such constituents near $x \approx \frac{1}{3}$.

## II. Vector **and axial** vector currents

The basic lagrangian describing hadronics systems is given by quantum chromodynamics (QCD),

$$\mathcal{L}_{QCD} = \sum_q \bar{q}\left[i\gamma^\mu\left(\partial_\mu + ig_s\sum_a \frac{\lambda^a}{2}\mathcal{A}^a_\mu\right) - m_q\right]q - \frac{1}{4}\sum_a \mathcal{F}^a_{\mu\nu}\,\mathcal{F}^{a,\mu\nu}. \qquad (3)$$

It describes the interaction of quarks (Dirac spinors q with 6 flavours and 3 colours) and gluons (vector potenial A, and field tensor $\mathcal{F}_{\mu\nu}$). The quantities $\lambda^a$ are the $SU(3)$ Gell-Mann matrices operating in colour space, with a = 1, 2 ...8. The round bracket on the *rhs* defines a covariant derivative involving the strong coupling constant g,. (It has been constructed in analogy to the more familiar gauge invariant coupling in quantum electrodynamics (QED), $\partial_\mu \rightarrow \partial_\mu + ieA_\mu$, in order to leave the lagrangian constant under a local gauge transformation of both the particle and the electromagnetic field.) If we restrict the discussion to low energy phenomena, only the 3 lightest quarks are important, with flavours $u$, d and $s$ and corresponding masses $m_u \approx 5MeV, m_d \approx 9MeV$ and $m_s \approx 120MeV$. Since these masses are nearly negligible on the hadronic scale ($m \approx 940MeV$), the QCD lagrangian is (nearly) invariant under a series of gauge transformation leading to 8 conserved vector and axial currents,

$$\begin{aligned} \mathcal{J}^a_\mu &= \bar{q}\gamma_\mu\frac{\lambda^a}{2}q \qquad (4)\\ \mathcal{J}^a_{5\mu} &= \bar{q}\gamma_\mu\gamma_5\frac{\lambda^a}{2}q, \end{aligned}$$

where $\lambda^a$ is now one of the 8 Gell-Mann matrices in

flavour space ($SU(3)$ of u, d and $s$ quarks). In addition, we can define a ninth quantitiy $\lambda^0$ as a diagonal matrix and corresponding vector and axial currents. It turns out, however, that the "ninth" axial current is not conserved, not even in the limit of vanishing quark masses, but determined by the gluon field ('$U_A(1)$ problem'),

$$\partial^\mu \mathcal{J}^0_{5\mu} = \frac{3}{64\pi^2} g_s^2 \epsilon_{\alpha\beta\gamma\delta} \mathcal{F}_c^{\alpha\beta} \mathcal{F}_c^{\gamma\delta}. \qquad (5)$$

In terms of these quantities the photon couples to the vector current

$$\mathcal{J}^{(\gamma)}_\mu = \mathcal{J}^3_\mu + \frac{1}{\sqrt{3}} \mathcal{J}^8_\mu, \qquad (6)$$

corresponding to a superposition of isovector (a = 3) and isoscalar (a = 8) vector currents in the more traditional language. Obviously, this current is conserved. The $\mathcal{Z}'$, on the other side, couples to a superposition of vector and axial currents as is typical for weak interactions. Moreover, it involves a linear combination of the currents with a = 3, 8 and 0. As a consequence of eq. (5) the weak neutral current coupling to the $\mathcal{Z}'$ gauge boson is not conserved.

$$\partial^\mu \left( \mathcal{J}^{(\mathcal{Z}')}_\mu + \mathcal{J}^{(\mathcal{Z}')}_{5\mu} \right) \neq 0. \qquad (7)$$

On the microscopic level the standard model (SM) predicts the structure of the currents in terms of quarks[1,2],

$$\mathcal{J}^{(\gamma)}_\mu = \frac{2}{3} \bar{u} \gamma_\mu u - \frac{1}{3} (\bar{d} \gamma_\mu d + \bar{s} \gamma_\mu s) \qquad (8)$$

$$\mathcal{J}^{(\mathcal{Z}')}_\mu = \left( \frac{1}{4} - \frac{2}{3} \sin^2 \theta_W \right) \bar{u} \gamma_\mu - \left( \frac{1}{4} - \frac{1}{3} \sin^2 \theta_W \right) (\bar{d} \gamma_\mu d + \bar{s} \gamma_\mu s), \qquad (9)$$

where $sin^2\theta_W = 0.2325 \pm 0.0008$ ('Weinberg angle'). Though we cannot calculate the nucleon wave functions directly from quarks and gluons, we can parametrize the general Lorentz structure of the nucleon's currents in terms of form factors[3],

$$\langle \vec{p'} | \mathcal{J}_\mu | \vec{p} \rangle = \bar{u}(\vec{p}) \left( F_1 \gamma_\mu + i \frac{F_2}{2m} \sigma_{\mu\nu} q^\nu \right) u(\vec{p}), \qquad (10)$$

$$\langle \vec{p'} | \mathcal{J}_{5\mu} | \vec{p} \rangle = \bar{u}(\vec{p'}) \left( G_A \gamma_\mu + \frac{G_P}{2m} q_\mu \right) \gamma_5 u(\vec{p}), \qquad (11)$$

where $u(\vec{p})$ and $\bar{u}(\vec{p'})$ are the spinors of the nucleon in the initial and final state, respectively. The electromagnetic current involves the familiar Dirac ($F_1$) and Pauli ($F_2$) form factors, the axial current the usual axial ($G_A$) and induced pseudoscalar ($G_P$) form factors. The form factors are functions of momentum transfer, $F_1 = F_1(Q^2)$ etc., normalized in the limit $Q^2 \to 0$ for protons (p) and neutrons (n) by

$$F_1^p \to 1 \qquad F_1^n \to 0 \qquad (12)$$

$$F_2^p \to \kappa_p = 2.79 \qquad F_2^n \to \kappa_n = -1.91$$

$$G_A \to g_A = 1.26 \qquad G_P \approx \frac{4m^2}{m_\pi^2 + Q^2} G_A.$$

The last of these relations follows from PCAC and pole dominance.

In general the momentum transfer $q^2 = w^2 - \vec{q}^2 = -Q^2$ involves the transfer of both energy and 3-momentum. We may choose, however, a particular frame of reference with zero energy transfer, the so-called 'Breit' or 'brickwall' system. In the simplest kinematical situation specified by that system, the nucleon comes in with momentum $-\vec{q}/2$ and, after absorbing the virtual photon with 3-momentum $\vec{q}$, is reflected with momentum $+\vec{q}/2$. In the case of elastic scattering, the nucleon's energy in both the inital and final state is then $E_i^B = E_f^B \equiv \sqrt{m^2 + \vec{q}^2/4}$, and the photon transfers no energy, $w = w^B = 0$. If we evaluate the Dirac

spinors of eq. (10) in that particular system, we obtain

$$\langle \vec{p}'|\mathcal{J}_\mu|\vec{p}\rangle = (\rho, \vec{\mathcal{J}}) = \left(F_1 - \tau F_2,\ i\,\frac{\vec{\sigma}\times\vec{q}}{2m}(F_1+F_2)\right), \tag{13}$$

which looks like the expression for a nonrelativistic particle with ar. electric charge and a magnetic moment given by the form factors

$$\begin{aligned} G_E(Q^2) &= F_1(Q^2) - \tau F_2(Q^2) \\ G_M(Q^2) &= F_1(Q^2) + F_2(Q^2), \end{aligned} \tag{14}$$

where $\mathbf{r} = Q^2/4m^2$ is a measure for the relativistic effects. Independent of the particular frame of reference, we refer to these linear combinations of the Dirac and Pauli form factors as the electric (E) and magnetic (M) 'Sachs form factors'. In the Breit frame, however, we may go one step further and interpret the form factors as Fourier transforms of a spatial distribution of charge or magnetization. In particular we have

$$\begin{aligned} G_E(Q^2) \to G_E(\vec{q}^{\,2}) &= \int \rho(\vec{r})\,\frac{\sin(|\vec{q}|r)}{|\vec{q}|r}\,d^3r \\ &= \int \rho(\vec{r})d^3r - \frac{\vec{q}^{\,2}}{6}\int \rho(\vec{r})r^2 d^3r + [\vec{q}^{\,4}]. \end{aligned} \tag{15}$$

Normalizing the charge density to 1 in the case of the proton, the second integral on the *rhs* defines the charge radius $r_E = \sqrt{\langle r^2\rangle_E}$ ('root-mean-square radius', *rms* radius). Quite generally we may define a radius by the first coefficient of a Taylor expansion of the form factor about $Q^2 = 0$.

## III. Inclusive polarized response

In the case of elastic electron scattering via photon exchange it is straightforward to evaluate the Feynman graph of Fig. 1 using eq. (10). The differential cross section is given by a current-current interaction[3],

$$d\sigma \sim |\sum_\mu j_\mu(e)\mathcal{J}^\mu(N)|^2 \sim \sum_{\mu\nu} j^*_\mu j_\nu \mathcal{J}^{\mu *}\mathcal{J}^\nu = \sum \eta_{\mu\nu}W^{\mu\nu}. \tag{16}$$

Summing over the electron spin in the final state and neglecting the mass of the electron, we obtain for the Lorentz tensor of the electron

$$\eta^{\pm}_{\mu\nu} = \eta^{(s)}_{\mu\nu} \pm \eta^{(a)}_{\mu\nu} \sim \frac{1}{2}\,[(k+k')_\mu(k+k')_\nu + g_{\mu\nu}q^2] \pm i\epsilon_{\mu\nu\alpha\beta}k^\alpha k'^\beta, \tag{17}$$

the two signs referring to the helicity $h = \pm\frac{1}{2}$ of the incoming electron. We note that the helicity dependent part of the tensor is antisymmetrical under the exchange of $\mu$ and $\nu$ by the properties of the Levi-Cività tensor $\epsilon_{\mu\nu\alpha\beta}$. If we sum over the polarization of the incident electron, only the term in the square bracket remains, which is a symmetrical tensor. The evaluation of the hadronic tensor $W_{\mu\nu}$ proceeds in a similar way. Except for the appearance of additional mass terms, the structure of the symmetrical tensor $W^{(s)}_{\mu\nu}$ is given by the two contributions in the square bracket of eq. (17), multiplied by the two form factors $G_E$ and $G_M$. The additional antisymmetrical tensor $W^{(a)}_{\mu\nu}$ appears only if the target nucleon is polarized (or if the polarization

of the recoiling nucleon is observed). As a consequence the differential cross section has the structure

$$d\sigma \sim \sum_{\mu\nu} \left( \eta^{(s)}_{\mu\nu} W^{\mu\nu,(s)} + \eta^{(a)}_{\mu\nu} W^{\mu\nu,(a)} \right), \qquad (18)$$

and the antisymmetrical tensors contribute only if both the incident electron and the target nucleon are polarized.

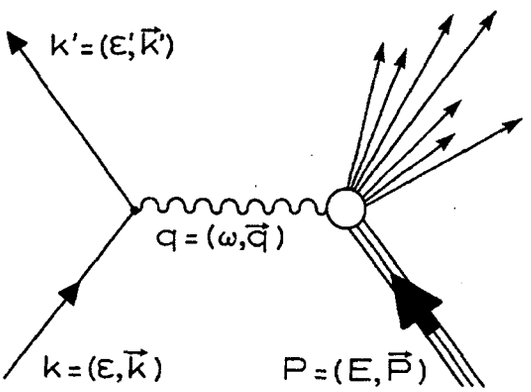


Figure 1: The kinematic variables for inclusive lepton scattering off a nucleon with $P^2 = m^2$. The final hadronic state has four-momentum $P' = P + q$ and total *c.m.* energy $W$ defined by $s = W^2 = (P+q)^2$. The quantity $Q^2 = -q^2 > 0$ for electron scattering, it vanishes for the absorption of real photons.

In the case of weak neutral currents, the exchanged $Z'$ boson couples to a superposition of vector and axial vector, e. g.

$$\langle k'|j_\mu + j_{5\mu}|k\rangle = \bar{u}(k')\gamma_\mu(1+\gamma_5)u(k) \qquad (19)$$

at the electronic vertex, and the equivalent combination of eqs. (10) and ( 11) at the hadronic vertex. Since the effect of weak neutral currents is very small, only the linear interference terms with photon exchange have to be taken into account. In addition to the tensor of eq. (17), there appears a parity violating term

$$\tilde{\eta}^{\pm}_{\mu\nu} = j^*_{5\mu} j_\nu = \tilde{\eta}^{(a)}_{\mu\nu} \pm \tilde{\eta}^{(s)}_{\mu\nu}. \qquad (20)$$

The symmetrical and antisymmetrical tensors have the same structure as in eq. (17), except that they have been interchanged and multiplied with the coupling constants of the weak interaction. Due to the pseudoscalar nature of the additional $\gamma_5$, the antisymmetrical tensor appears now in the spin-independent part and the symmetrical tensor changes sign depending on the helicity of the electron. The leading contributions to the total cross section,

$$d\sigma^{\pm} \sim \sum \eta^{(s)}_{\mu\nu} W^{\mu\nu,(s)} \pm \sum \tilde{\eta}^{(s)}_{\mu\nu} \tilde{W}^{\mu\nu,(s)} \pm \sum \tilde{\eta}^{(a)}_{\mu\nu} \tilde{W}^{\mu\nu,(a)}, \qquad (21)$$

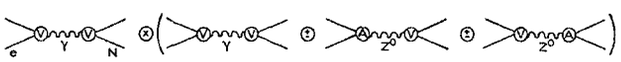


Figure 2: The leading order contributions to the differential cross section for parity-violating electron scattering. The electromagnetic scattering with photons ($\gamma$) attached to the vector currents (V) of electron *(e)* and nucleon (N) interferes with either photon exchange or $Z'$ exchange, the $Z'$ attached to the vector current of the electron and the axial current *(A)* of the nucleon *or* to the axial current of the electron and the vector current of the nucleon. The latter two terms change sign with the helicity of the electron.

have been shown in Fig. 2. The two interference terms of y and $Z'$ exchange change sign if the helicity of the electron is flipped. They give information on the axial form factor $G_A$ of the nucleon and on its electric ($\tilde{G}_E$) and magnetic ($\tilde{G}_M$) form factors as seen by the $Z'$. Note that these form factors are different from the values $G_E$ and $G_M$ seen by the photon because of the different coupling of the two particles to the quarks (see eqs. (8) and (9)).

An evaluation of the electronic tensors $\eta_{\mu\nu}$ in the laboratory frame leads to the familiar kinematical functions appearing in a generalized Rosenbluth decomposition of the cross section[4]

$$v_L = Q^4/\vec{q}^{\,4}, \qquad v_T = Q^2/2\vec{q}^{\,2} + \tan^2(\theta/2) \qquad (22)$$
$$v'_T = \tan(\theta/2)\sqrt{Q^2/\vec{q}^{\,2} + \tan^2(\theta/2)},$$

where $v_L$ and $v_T$ correspond to the two structures in $\eta^{(s)}_{\mu\nu}$ and $v_{T'}$ is derived from $\eta^{(a)}_{\mu\nu}$. The most general form of the cross section has been discussed in ref. [4].

## III. The form factors of proton and neutron

The differential cross section for the scattering of unpolarized electrons off the nucleon is[3]

$$d\sigma = \frac{d\sigma_+ + d\sigma_-}{2} \sim \frac{G_E^2 + \tau G_M^2}{1+\tau} + 2\tau \tan^2\frac{\theta}{2}\, G_M^2. \tag{23}$$

The two form factors can be determined by means of a 'Rosenbluth plot', showing the cross section as function of $\tan^2\frac{\theta}{2}$ for constant $Q^2$. The data should lie on a straiglit line with a slope $\tau G_M^2$, and the extrapolation to the (unphysical) point $\tan^2\frac{\theta}{2} = -\frac{1}{\tau}$ determines the electric form factor $G_E$. Unfortunately, this procedure has a limited range of applicability. For decreasing $Q^2$, also $\tau$ and the slope become small and the error bars on $G_M^2$ increase. Large $Q^2$, on the other hand side, leads to a small electric contribution $\sim G_E^2/\tau$ with large errors for the electric form factor. In the case of the proton, the Rosenbluth plot has now been evaluated up to $Q^2 = 8.8\mathrm{GeV}^2$ in the experiment NE−11 at $SLAC$[5]. The results are shown in Fig. 3. Additional and more precise information will be obtained at the new electron accelerators by double polarization experiments (the antisymmetrical-antisymmetrical terms in eq. (18)!), in particular target polarization $\vec{p}(\vec{e},e')p$ at small $Q^2$ and recoil polarization $p(\vec{e},e')\vec{p}$ at large $Q^2$. The additional transverse-longitudinal interference terms in such polarization exprriments contain terms $\sim G_E G_M$ rather tlian the sum of squares as in the unpolarized cross section, eq. (23). Of particular interest is a recoil polarization of the proton perpendicular (sideways) to the momentum tritnsfer $\vec{q}$ and in the scattering plane.

The situat on is much more delicate in the case of the neutron. Since its overall charge vanishes, $G_E^n(0) = 0$ and $G_E^n$ remains small at all $Q^2$. Moreover, there are no neutron targets available and the form factors have to be determiiied from scattering off the deuteron (or other light nuclei). The only reliable experimental data up to now are from scattering of neutrons off atomic electrons. For obvious kinematical reasons, only small values of $Q^2$ can be obtained in such experiments. The result is a very accurate slope of the form factor at $Q^2 = 0$, i. e. a neutron radius ($r^2$);. In order to obtain information at the higher $Q^2$, two techniques have been used up to now:

**(I)** Quasifree scattering off the deuteron determines the incoherent sum of proton and neutron contributions[6]. The prescription

$$\left(|G_E^p|^2 + |G_E^n|^2\right)_{deut} - |G_E^p|^2_{prot} = |G_E^n|^2 \tag{24}$$

leads to big uncertainties for the neutron from factor, because the structure of the proton in the deuteron has to be corrected by final state interactions, correlations, meson exchange and relativistic effects of the order of 20%. Since $G_E^n \ll G_E^p$, we expect large systematical errors.

**(II)** Elastic scattering off the deuteron[7], leading to the cross section

$$\sigma_{ed} \sim (G_E^p + G_E^n)^2 \cdot F_{deut}^2 + \text{corrections}. \tag{25}$$

Again we find large model dependencies. The deuteron form factor $F_{deut}$ depends on the specific nucleon-nucleon potential, and also the corrections (meson exchange, relativistic and off-shell effects) are expected to be large, introducing systematical errors of the order of 30 − 50%.

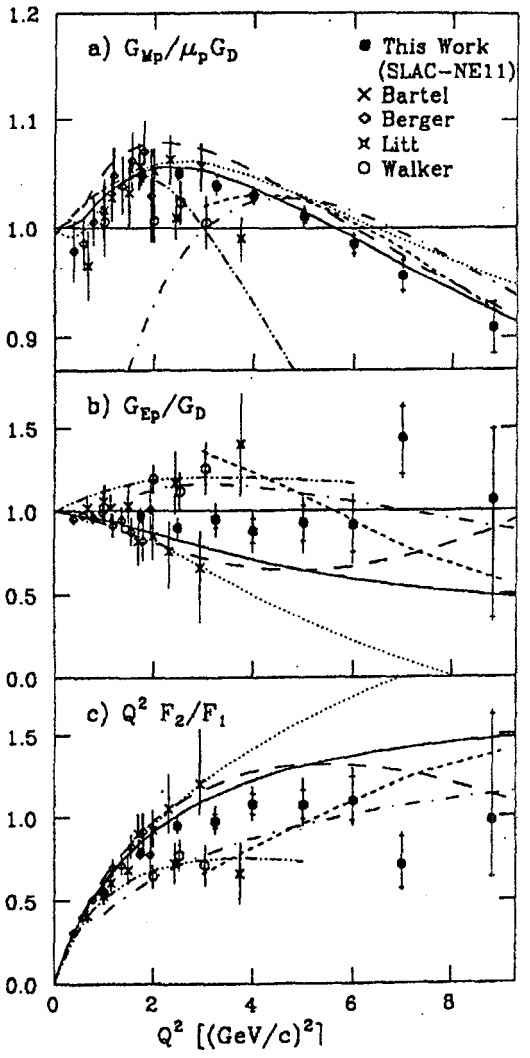


Figure 3: The form factors of the proton. Top: Magnetic form factor $G_M^p$ normalized to the dipole form factor $G_D$ (see text), middle: electric form factor $G_E^p$ normalized to $G_D$, bottom: the ratio $Q^2F_2/F_1$ expected to approach a constant for $Q^2 \to \infty$. The predictions are from various vector dominance models and QCD sum rules (dashed-dotted curve). References to the data and theoreticai predictions see Bosted et al[5].

Within the large error bars of present experiments, the data follow surprisingly close the so-called 'dipole fit' for the Sachs form factors[6],

$$\begin{aligned} G_E^p &= G_M^p/\mu_p = G_M^n/\mu_n = (1+Q^2/M_V^2)^{-2} \\ G_E^n/\mu_n &= -\tau(1+Q^2/M_{V'}^2)^{-1}(1+Q^2/M_V^2)^{-2}, \end{aligned} \tag{26}$$

with $\mu_p = 2.79$, $\mu_n = -1.91$, m = $940MeV$, $M_V = 840MeV$ and $M_{V'} = 790MeV$. Since r = $Q^2/4m^2$, $G_E^n(0)$ vanishes, while $G_E^p(0) = 1$ and the magnetic form factors approach the total magnetic moments for $Q^2 \to 0$. In the asymptotic region, $Q^2 \to \infty$, all Sachs form factors have a $Q^{-4}$ behaviour as expected from perturbative (asymptotic) QCD (see below). In order to get an idea about the size of the form factors, we have sketched the predictions of the dipole fit for the neutron in Fig. 4. The corresponding results for the proton are simply obtained by a scaling of $G_M^n$. We note in particular that $G_E^n$ is quite small over the whole range of momentum transfer.

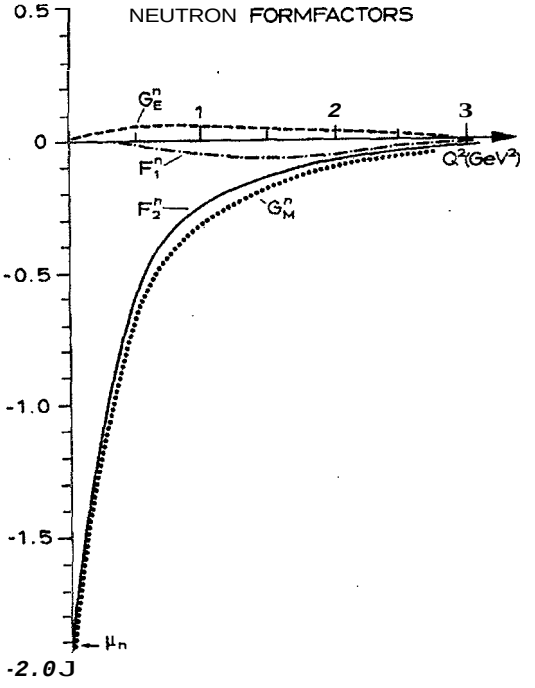


Figure 4: The form factors of the neutron as function of $Q^2$ as obtained from the dipole fit, eq. (26). See text for definitions.

Why are we so interested in the form factors of the nucleon ? The reason is that they can be measured in a well-defined way and, at the same time, provide a critical test of our models of the nucleon. Moreover, the Fourier transform of these form factors gives us some idea about the distribution of charge and magnetization inside a nucleon. Let us briefly discuss, therefore, some of the models and their predictions.

### IV.1 Perturbative QCD (PQCD)

In the limit of $Q^2 \to \infty$ the nucleon should be described by the 'minimal' configuration of 3 quarks. Since the photon strikes only one of these quarks, the

two others have to be 'informed' about the scattering process by 2 gluon 'messengers' (see Fig. 5). Each of these gluons has the propagator of a massless particle, $Q^{-2}$, the excliange of two of them leads to a $Q^{-4}$ behaviour of the form factor[8]. If we solve eqs. (14) for the form factors $F_1$ and $F_2$, we find $F_1 \rightarrow Q^{-4}$ and $F_2 \rightarrow Q^{-6}$ in the asymptotic limit, i. e. the Pauli form factor drops faster than all others due to the spin flip involved. There are some indications of this scaling in the lower part of Fig. 3.

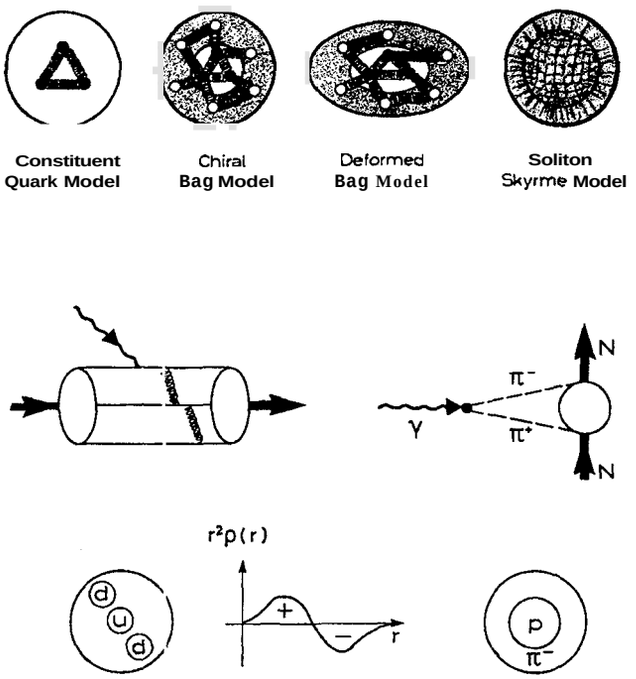


Figure 5: Top: Phenomenological models of the nucleon in terms of quarks, coexisting quark and pion phases, and a pure meson fielc!. Middle: The nucleon as a 3 quark system in *PQCD* (left). Elastic scattering requires the exchange of two gluons (internal wavy lines). Dispersion relations connect the photon with all possible intermediate states starting with a two-pion or three-pion system for its isovector or isoscalar component, respectively (right). Bottom: Both the *CQM* with hyperfine interaction (left) and the CBM (right) can describe the observed charge distribution in the neutron: a positive core surrounded by a negative cloud.

## PV.2 Diquark correlations

At intermediate momentum transfer corrections to PQCD should become increasingly important. These involve correlations between the quarks in the wave function or at the operator level. (Some authors even suspect that such correlations give the dominant contributions also at very high $Q^2$). A particularly convenient way to obtain such terms is to introduce strong diquark correlations[9], i.e. the nucleon is reduced to a two-body problem of a diquark and a quark in a potential. Such corrections to the asymptotically leading terms are called 'higher twist'. They make it possible to calculate the Pauli form factors $F_2$, which vanishes in PQCD.

## N.2 Nonperturbative models

In the range of $Q^2 \leq 1\text{GeV}^2$ the interaction between the quarks cannot be treated in a perturbative manner. Instead, various models have been developed to describe the basic symmetries of QCD in a phenomenological way (see Fig. 5). The constituent quark model(*CQM*) assumes that 3 heavy ('constituent') quarks are confined by a common potential. In the ground state of such a system the quarks move in a symmetrical S−state, their spins and flavours (u and d) are coupled to a symmetrical configuration according to $SU(6) = SU(2)_{spin} \times SU(3)_{flavour}$, and the colour degree of freedom provides the overall antisymmetry required by the Pauli principle. In such a'scheme, u and d quarks move in the same orbits and have the same (matter) density distribution, $\rho_u(\vec{r}) = \rho_d(\vec{r})$. As a consequence the two d quarks of the neutron carry exactly the opposite charge distribution as the u quark, the charge distribution of the neutron vanishes at each point in space, and $G_E(Q^2) = 0$ for all values of momentum transfer.

A more realistic description is obtained by introducing a hyperfine interaction due to the exchange of gluons between the quarks[10,11]. Such a force admixes higher orbitals into the ground state wave function. In addition to the lowest symmetrical S−state (admixture coefficient as) we find an excited symmetrical S−state ($a_{S'}$), a state of mixed symmetry ($a_M$) leading to $\rho_u \neq \rho_d$, and a very small $D$−state ('bag- deformation', $a_D$). If the force is fitted to the excitation spectrum of the nucleon, we obtain the neutron charge radius

where $\alpha_0$ is the oscillator parameter describing the range of the confining (oscillator) potential. The negative sign of $\langle r^2\rangle_E^n$ reflects the fact tliat the two d quarks (charge $-1/3$) move in a slightly larger orbit tlian the u quark (charge $+2/3$). In a simple picture the neutron lias a core of positive charge surrounded by a negatively charged cloud (see Fig. 5). Experimentally, the present data indicate $\langle r^2\rangle_d \approx 0.68 fm^2$ and $\langle r^2\rangle, \approx 0.51\mathrm{fm}^2$.

Chiral bag models (CBM) describe the nucleon as a (small) quark bag coexisting with a surrounding pion cloud. The coupling between the two phases is constructed such that chiral symmetry (PCAC) is conserved. Without the pion cloud we obtain the MIT bag model of u and d quarks in a central potential, leading to $G_E^n = 0$ as in the case of the CQM without hyperfine interaction. However, the pion-quark interaction leads to an admixture of a configuration with a proton bag in the centre of tlie nucleon and a cloud of negatively charged pions[12,13]. Another description is the Nambu-Jona-Lasinio model (NJL), which starts from a nonlinear, chirally invariant lagrangian between essentially massless quarks[14]. The nonlinear interaction generates the mass of the quarks and, at the same time, creates the pion as a strongly bound quark-antiquark pair.

A completely opposite approach is taken in soliton models, solutions of a nonlinear lagrangian of meson fields[15]. This projection of QCD on purely mesonic degrees of freedom is justified in the limit of $N_c \to \infty$, where $N_c$ is the number of colours. Since $N_c = 3$ in nature, the success of this model is surprising. It is probably due to the incorporation of certain aspects of vector dominance (VMD, see below) by explicity introducing $\rho$ and w mesons and their coupling to the photon. The radius of the nucleon in these models is described by the fact that the photon couples to both the vector meson with mass $M_V$ and the (small) soliton bag,

$$\langle r^2\rangle = \frac{6}{M_V^2} + \langle r^2\rangle_{bag} \approx (0.4 + 0.3) fm^2. \qquad (28)$$

In view of the different physics behind the models, their overall agreement with the data is quite satisfactory. A detailed study of the predictions (see table 1) shows, however, that none of the models is able to describe all radii at the same time at the 10% level.

### **IV.4** Dispersion relations

Using Lorentz invariance, gauge invariance and causality (analyticity), it is possible to derive dispersion relation for the form factors[16]. In a somewhat symbolic way,

$$G(Q^2) = \int_{t_0}^{\infty} dt \frac{f(t)}{t+Q^2} \to \sum_V \frac{a_V}{1+Q^2/M_V^2} \quad , \qquad (29)$$

where $t_0$ is the threshold for the lowest state appearing in the t- channel (see Fig. 5). In case of the isovector component of the photon, this threshold is given by the mass of two pions, $t_0 = (2m_\pi)^2$. Experimentally one finds, however, that this amplitude is quite small close to threshold and dominated by the $\rho$-meson. Similarly the isoscalar photon has a threshold at $t_0 = (3m_\pi)^2$ and is dominated by the w-meson. It is convenient, therefore, to parametrize the integral by a sum of poles at the positions of the vector mesons (vector meson dominance, VMD). Unfortunately, however, the analysis of the data requires a second pole close to the mass of the $\rho$ or w and with negative residuum, in order to describe the phenomenological dipole fit. The origin of this second pole is yet kind of a puzzle, and a more realistic treatment of the dispersion integral in eq. (29) is absolutely required.

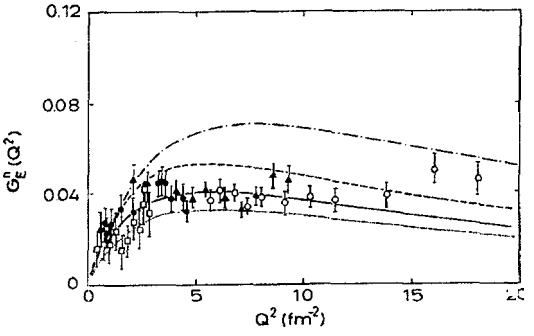


Figure 6: The electric form factor $G_E^n(Q^2)$ of the neutron derived by an analysis using the Paris potential (data normalized to the full line)[7]. Other curves correspond to different choices of the potential, the highest curve shown is for the Nijmegen potential.

Why do we want to see new and better experiments? As has been shown in Fig. 6, even the most recent high quality data for scattering on the deuteron suffer

Table 1: The electric radii of proton and neutron, $\langle r^2\rangle_E^{p,n}$, and the axial radius of the proton, $\langle r^2\rangle_A^p$. The experimental data are compared to some theoretical predictions, in units of $fm^2$.

| | $\langle r^2\rangle_E^p$ | $\langle r^2\rangle_E^n$ | $\langle r^2\rangle_A^p$ |
|---|---|---|---|
| experiment | .74 | -.12 | .39 |
| CQM[11] | .74 | -.10 | |
| MIT bag[12] | .53 | 0 | .35 |
| CBM[12] | .66 | -.13 | .28 |
| CBM $+N^*, \Delta \ldots$[13] | .73 | -.15 | .27 |
| NJL, $m_q = 418$[14] | .60 | -.12 | |
| Soliton[15] | .96 | -.25 | .38 |

from large systematical errors. In spite of their good statistical accuracy, the analysis depends on the choice of the nucleon-nucleon potential for the analysis of the deuteron, the best neutron target we have. This model analysis of the data has a large error band of the same range as the theoretical predictions for the neutron form factor shown in Fig. 7. Clearly, the corresponding charge distributions given in Fig. 8 differ wildly, and yet we cannot exclude any of them by the existing data. As has been poiiited out earlier, the experimental breakthrough is expected to come by polarization transfer. It lias been shown for quasifree scattering off the deuteron that there exist kinematical situations for which meson exchange currents, final state interactions and other binding effects can be safely neglected[17]. This is particularly true for forward emitted neutrons with recoil polarization perpendicular to their momentum and in the scattering plane. In these cases the observed polarization trarsfer should be essentially proportional to tlie neutron form factor $G_E^n$.

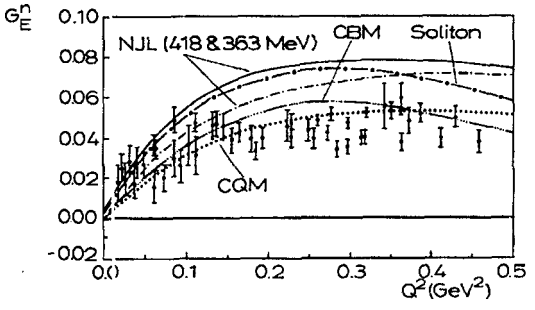


Figure 7: The electric form factor $G_E^n(Q^2)$ of the neutron compared to different predictions as described in the text and in table 1. Data: as in Fig. 6.

Experiments to determine $G_E^n$ by the reaction $\vec{d}(\vec{e}, e'n)$, $d(\vec{e}, e'\vec{n})$ and ${}^3\vec{H}e(\vec{e}, e'n)$ are underway at $MIT$/Bates[18,19] and MAMI[20] in the region up to $Q^2 = 0.6GeV^2$. Some preliminary results from Mainz indicate that the neutron form factor could be substantially larger than derived from elastic scattering off the deuteron. At higher momentum transfer up to $Q^2 = 2\text{GeV}^2$, two experiments are being planned at $CEBAF$[21,22].

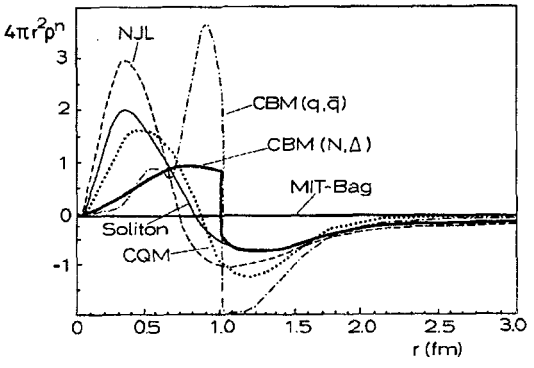


Figure 8: Predicted charge distributions $\rho_{(r)}^n$ of the neutron. Models as in fig. 7.

## V. The strangeness content of the nucleon

The basic interest in parity-violating electron scattering is due to fact that we hope to learn about the content of strange-antistrange quark pairs in the nucleon[23]. This possibility arises because the photon and the $Z^0$ boson couple to the vector currents of the quarks in a different way. The corresponding charges of the quarks can be read off eqs. (8) and (9). If we approximate the Weinberg angle by $\sin^2\theta_W \approx \frac{1}{4}$ and leave out the overall coupling constants of the electromagnetic and the weak interaction, the photon sees the quark charges $e_u = \frac{2}{3}$ and $e_d = e_s = -\frac{1}{3}$, while the $Z^0$ boson couples with $\tilde{e}_u \approx \frac{1}{12}$ and $\tilde{e}_d = \tilde{e}_s \approx -\frac{1}{6}$.

In addition to the differential cross section of eq. (23), da $= (d\sigma^+ + d\sigma^-)/2$, a polarization experiment will also determine the asymmetry[24],

$$A = (d\sigma^+ - da-)/(da+ + da-) \sim \frac{\left[\frac{G_E\tilde{G}_E+\tau G_M\tilde{G}_M}{1+\tau} + 2\tau G_M\tilde{G}_M \tan^2\frac{\theta}{2} + \text{const.}\,(1-4\sin^2\theta_W)G_M\tilde{G}_A\right]}{\left[\frac{G_E^2+\tau G_M^2}{1+\tau} + 2\tau G_M^2\tan^2\frac{\theta}{2}\right]} \quad (30)$$

In comparing with eqs.(20) and (21) we note that the first two contributions in the numerator arise from an axial coupling at the electron vertex and a vector coupling of the $Z^0$ to the nucleon. The third term describes the opposite case, vector coupling to the electron and axial coupling to the nucleon. It is strongly suppressed by a factor $(1-4\sin^2\theta_W) \approx 0$ appearing at the electron vertex. If the electromagnetic form factors are known, we may determine 3 new form factors by a generalized Rosenbluth plot,

$$A = A_E(\tilde{G}_E) + A_M(\tilde{G}_M) + A_A(\tilde{G}_A). \quad (31)$$

These 3 contributions have been shown in Fig. 9 for the kinematics available at a $1GeV$ accelerator. The predicted value for $A_E$ is very small and requires a precision measurement at forward angles (small momentum transfer). At angles $\theta \geq 15°$ the magnetic term $A_M$ is by far the dominant one, the smallness of the weak charge of the electron will make it difficult to extract the axial form factor $\tilde{G}_A$.

Once the weak neutral form factors have been measured, it will he straightforward to determine the strangeness content of the nucleon. Of course, we cannot (yet) calculate the form factors of the nucleon directly from eqs. (8) and (9). However, we observe that the quark currents $\bar{u}\gamma_\mu u$ appearing in these equations will lead to the same matrix element in both cases and, hence, to the same contribution $G_u$ of the u quarks to the form factors. In the case of the proton this contribution includes both the 2 valence quarks and the a priori unknown $u\bar{u}$ sea quarks. Similarly we define $G_d$ for the d quark plus dd sea quarks, and G, for the $s\bar{s}$ sea quarks. Furthermore we assume that the neutron is obtained by changing the isospin, i. e. $G_u \leftrightarrow G_d$. In this way we obtain the equations

$$\begin{aligned} \gamma p: \quad G^p &= \frac{2}{3}G_u - \frac{1}{3}G_d - \frac{1}{3}G_s \quad (32)\\ \gamma n: \quad G^n &= \frac{2}{3}G_d - \frac{1}{3}G_u - \frac{1}{3}G_s \\ Z^0 p: \quad \tilde{G}^p &= \left(\frac{1}{4} - \frac{2}{3}s^2\right)G_u + \left(-\frac{1}{4} + \frac{1}{3}s^2\right)(G_d + G_s), \end{aligned}$$

where $s^2 = sin^2\theta_W$. Eliminating the $u$ and d quarks from these equations, we can relate the strangeness content G, directly to the observables,

$$\begin{aligned} \tilde{G}^p &= \frac{1}{4}\left[(1-4s^2)G^p - G^n - G^s\right] \quad (33)\\ \tilde{G}^n &= \frac{1}{4}\left[(1-4s^2)G^n - G^p - G^s\right]. \end{aligned}$$

In case of an atomic nucleus (mass number $A = N + Z$) the simplest model gives

$$\tilde{G}^{nucleus} = -\sin^2\theta_W A\frac{G^p+G^n}{2} + \frac{Z-N}{2}\frac{G^p-G^n}{2} - \frac{1}{4}AG^s. \tag{34}$$

Particular simple and promising targets are the proton and $^4He$. In the latter case N = Z = 2, and the wave function can be approximated by all 4 nucleons in an $S$-state. The asymmetry is then given by

$$A(^4He) = \frac{G_F Q^2}{\alpha\pi\sqrt{2}}\left(\sin^2\theta_W + \frac{G_E^s}{2(G_E^p+G_E^n)}\right), \tag{35}$$

where $G_F$ is the Fermi constant of the weak interaction. With the above approximation the asymmetry does not depend on the nuclear wave function. If both $G_E^p$ and $G_E^n$ have been determined previously, eq. (35) can be used directly to determine $G_E^s$.

The corresponding equation for the proton is much more involved due to the spin degree of freedom. It reads

$$A^p = -\frac{G_F m_p^2}{\sqrt{2}\pi\alpha}\tau\ \{(1-4s^2) - \frac{\epsilon G_E^p(G_E^n+G_E^s)+\tau G_M^p(G_M^n+G_M^s)}{\epsilon(G_E^p)^2+\tau(G_M^p)^2} + (1-4s^2)\sqrt{\tau(1+\tau)}\sqrt{(1-\epsilon^2)}\frac{G_M^p(G_A^p-G_A^n-G_A^s)}{\epsilon(G_E^p)^2+\tau(G_M^p)^2}\Big\}, \tag{36}$$

where $\varepsilon = (1+2(1+\tau)\tan^2\frac{\theta}{2})^{-1}$ is the transverse polarization of the virtual photon and $S = \sin\theta_w$. By appropriate measurements and a generalized Rosenbluth plot we may determine all 3 form factors of the strange quarks, their influence on the charge ($G_E^s$), the magnetization ($G_M^s$) and the axial current ($G_A^s$). For forward angles ($\theta \to 0, \varepsilon \to 1$) we should observe $G_E^s$ at small $Q^2$ (sniall $\tau$!). At the larger $Q^2$ (larger $\tau$!) GJ becomes the dominant quantity, while the axial term $G_A^s$ is suppressed by the factor $1-4\sin^2\theta_W$. Even though the last term becomes larger at backward angles ($\theta \to 180°, \varepsilon \to 0$), it will always be difficult to extract it from the data due to higher order (radiative) corrections[22].

Since there are no strange valence quarks in the nucleon, the net charge of the strange content vanishes,

$$G_E^s(Q^2) = 0 - \frac{Q^2\langle r^2\rangle_E^s}{6} + \ldots, \tag{37}$$

and the leading order term is given by the rms radius of the strange sea. Schematicmodels for the strangeness contribution are shown in Fig. 10. By means of a weak interaction the proton can decay into a $\Sigma^0$ or $\Lambda^0$ hyperon and a $K^+$. In this way a fraction of the positive charge of the proton is carried from the centre to a surrounding cloiid of positively charged $K$ mesons. On the quark level the interaction of the quarks via gluon exchange will easily lead to the creation of $s\bar{s}$ pairs. In order to obtain a finite radius $(r^2)\%$, it is however necessary that the pairs are spatially separated by additional correlations. If the $\bar{s}$ quarks move to the outer region and the s quarks remain in the centre as in Fig. 10, we obtain the same qualitative picture as in the case of $K^+$ production. As a consequence we expect $(r^2)_s > 0$ for the proton.

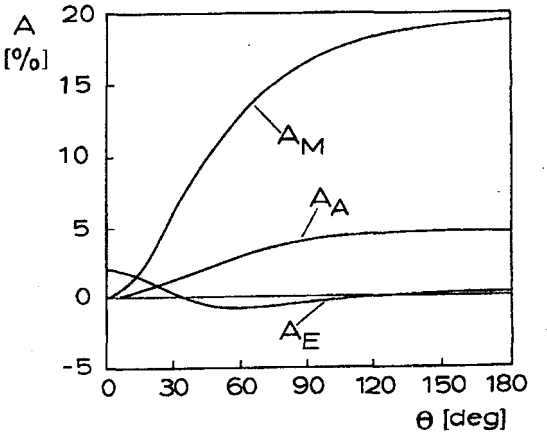


Figure 9: Relative contributions of the weak neutral form factors of the nucleon to the total asymmetry as a function of scattering angle $\theta$ for incident energy $\epsilon = 855 MeV$ [30]. The asymmetries are defined as in eqs. (30) and (31).

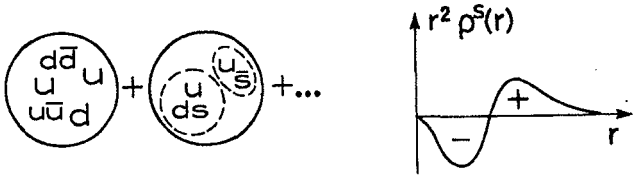


Figure 10: Models of the charge distribution of the proton carried by strange quarks, $\rho^s(r)$. Note that a concentration of strangeness in the centre and antistrangeness in the outer region of the proton leads to a positive value of $\langle r^2 \rangle_E^s$.

An estimate of the strangeness content has been given by Jaffe[25]. This model works particularly well in the case of the isoscalar photon whose response is strongly dominated by the $w$ at $780 MeV$ (see section IV, VMD). The next meson with the quantum numbers of the photon is the \$ at $1020 MeV$, which is nearly completely described by $s\bar{s}$ pairs. A fit to the form factors of the nucleon in the framework of the VMD and including the 4 gives

$$\langle r^2 \rangle_1^s = (0.16 \pm 0.06) fm^2 \qquad (38)$$
$$\kappa^s = -0.31 \pm 0.09$$

for the strange contribution to the *rms* of the Dirac form factor and to the anomalous magnetic moment.

In order to appreciate the difficulties of the experiment it is important to note that the factor in front of the bracket on the *rhs* of eq. (35) is of the order of $10^{-4}$ even at $Q^2 = 1 \mathrm{GeV}^2$. In the past such relations have been used to determine the Weinberg angle $\theta_W$, assuming that the strange contribution $G^s$ can be neglected. The first such measurement has been performed at *SLAC*[26] using a proton target, later experiments include quasifree scattering off Li at Mainz[27] and scattering off $^{12}C$ at *MIT/Bates*[28]. In the last case the momentum transfer has been only $Q^2 = (150 MeV)^2$, leading to the tiny asymmetry $A = (0.60 \pm 0.14 \pm 0.02) \cdot 10^{-6}$ and a value well compatible with other measurements of $\theta_W$. The strategy of the new experiments will be exactly opposite. Since $\theta_W$ is now known to about 3 decimal places, relations like eq. (35) can be safely used to determine $G^s$. Quite a few such experiments are being planned at the new electron accelerators. At *Bates/MIT* the SAMPLE collaboration plans to measure $\kappa^s$ at small $Q^2$ but large 8 [29], and the A4 collaboration at Mainz[30] intends to determine $\langle r^2 \rangle_E^s$ at small scattering angles. Finally, there are 3 big projects at CEBAF to extract the strangeness content of the nucleon by parity-violating electron scattering from both the proton[31,32], and $^4He$ [33], using the much larger kinematical leverage of the 4 – 6GeV accelerator. In view of the strongly differing predictions[25,34] on the strangeness content of the nucleon (Fig. 11) the result of these experiments will be invaluable for all model-builders.

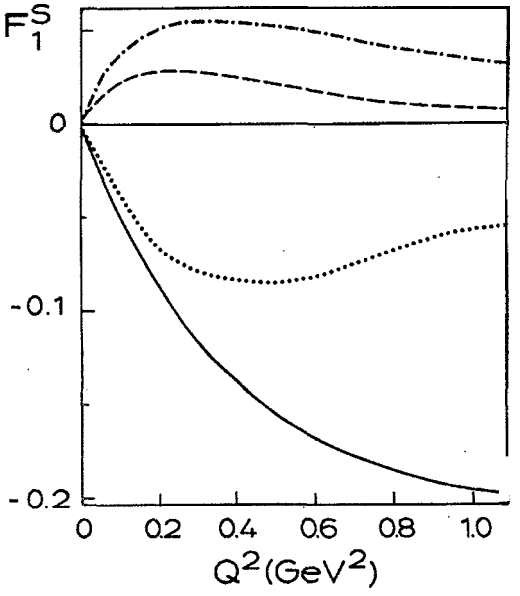


Figure 11: The strangeness contribution to the Dirac form factor $F_1^s$ as function of $Q^2$. Solid line: *VMD* fit to the proton data[25]; dashed-dotted and dotted line: Skyrme model without and with vector mesons[34]; dashed line: neutron form factor for comparison.

## VI. Deep inelastic scattering and spin structure

As has been shown in section I and illustrated in Fig. 1, the structure functions for inclusive inelastic scattering depend on two variables, the momentum transfer $Q^2$ and the total *c.m.* energy W (or, alternatively, the lab energy $\omega_L$ carried by the incident photon). The Bjorken variable x (see eq.(1) ) classifies the different reaction mechanisms, e.g. $x = 1$ for elastic scattering off the nucleon and $0 \leq x < 1$ for inelastic scattering[35]. Note that the condition $x = 1$ for elastic scattering fixes the energy (W, or $\omega_L$) in terms of $Q^2$, hence the nucleon form factors appearing in elastic scattering depend on

$Q^2$ only. In the case of deep inelastic scattering (DIS) we assume that the wave length of the virtual photon is so small that the reaction takes place on an individual constituent (parton) of the nucleon. If this parton is a truly structureless particle, the scattering off that parton will be essentially elastic scattering. In a nonrelativistic picture of constituent quarks, we expect such a scattering at $x = m_q/m_N \approx \frac{1}{3}$. Similarly, scattering off a virtual pion (quark-antiquark pair) will take place at $x = m_\pi/m_N \approx \frac{1}{7}$. In a relativistic description of *DIS*, the reaction may be analyzed in the so-called 'infinite momentum frame', in which x corresponds to the fraction of the nucleon's momentum carried by the struck parton. The probability to find a parton with such a momentum is denoted by $f_q(x)$, where q refers to the flavour (u, d, s) of the struck parton (quark).

Let us briefly compare the coherent nature of elastic scattering off the nucleon, which has been discussed in the previous sections, to the incoherent picture assumed in the case of DIS. In the case of elastic scattering, the cross section is

$$d\sigma_{el} \sim |\langle N|\sum_q e_q \mathcal{J}_\mu(q)|N\rangle|^2 \sim (e_u f_u + e_d f_d + e_s f_s)^2, \tag{39}$$

where $f_q$ are the matrix elements for the different flavour currents $\mathcal{J}_\mu$ in the ground state of the nucleon. Obviously, the process is fully coherent. In inclusive inelastic scattering, we have to sum over all the excited states of the nucleon (N*). Using closure we obtain

$$\begin{aligned} d\sigma_{inel} &\sim \sum_{N^*}\langle N^*|\sum_{q'}\mathcal{J}_\mu(q')|N\rangle^+\langle N^*|\sum_q e_q\mathcal{J}_\nu(q)|N\rangle \\ &\to \langle N|\sum_{q'q} e_{q'}e_q\mathcal{J}_\mu^+(q')\mathcal{J}_\nu(q)|N\rangle. \end{aligned} \tag{40}$$

In DIS we further assume that the correlations between different quarks ($q \neq q'$) vanish and that each scattering takes place on one parton only. In this approximation we obtain the extreme incoherent limit

$$d\sigma_{DIS} \sim e_u^2 f_\mu^{\mu\nu} + e_d^2 f_d^{\mu\nu} + e_s^2 f_s^{\mu\nu}, \tag{41}$$

where $f_q^{\mu\nu}$ are the expectation values of the Lorentz tensors $W_q^{\mu\nu} = (\mathcal{J}_{(q)}^\mu)^+\mathcal{J}_{(q)}^\nu$ in the ground state of the nucleon. As has been shown in the previous sections, there is only a limited number of such Lorentz tensors. In the case of the scattering of unpolarized electrons off unpolarized nucleons, there are two independent scalars, $\vec{\mathcal{J}}^+\cdot\vec{\mathcal{J}}$ and $\rho^+\cdot\rho$, corresponding to transverse and longitudinal currents and leading to the structure functions $F_1$ and $F_2$. In general these structure functions depend on two variables, e.g. $s$ and $Q^2$. In DIS, however, the additional dependence on $Q^2$ is assumed to be negligible ('scaling'). Moreover, the two structure functions may be expressed in terms of the momentum distribution $f_q(x)$[36,37,23]

$$\begin{aligned} F_1(x,Q^2) &\to^{DIS} F_1(x) = \frac{1}{2}\sum e_q^2 f_q(x) \\ F_2(x,Q^2) &\to^{DIS} F_2(x) = x\sum e_q^2 f_q(x). \end{aligned} \tag{42}$$

With polarization degrees of freedom we may construct two vectors, essentially $\vec{\mathcal{J}}^+ \times \vec{\mathcal{J}}$ and $\rho^+\vec{\mathcal{J}}$, leading to the polarized structure functions $G_1$ and $G_2$. In conclusion the cross section for the scattering of electrons with positive helicity (+) off nucleons with spins parallel (+) or antiparallel (−) to the spin of the electron has the structure[36,37]

$$\frac{d^2\sigma(+,\pm)}{d\Omega dE'} = \ldots(\ldots F_1 + \ldots F_2) \pm \ldots(\ldots G_1 + \ldots G_2), \tag{43}$$

where the ellipses denote well-defined kinematical factors. The 4 structure functions may be determined, in principle, by a 'super' Rosenbluth-plot. In practice, however, only the transverse functions have been studied, because the longitudinal effects tend to be small in the usual kinematical situations. Combining charged lepton and neutrino scattering data, it has been pos-

sible to measure the valence and sea quark contributions separately. It has been found, indeed, that the valence quark distribution peaks near x $\approx \frac{1}{3}$, while the sea quarks tend to give a substantial contribution for small $x$. Since the distribution functions $f_q(x)$ define the probability to find a quark with a certain fraction of the momentum of the nucleon, the integral is well defined in a model of constituent quarks only. For the integral

$$\int_0^1 F_2(x)dx = \sum_q e_q^2 \int_0^1 f_q(x)xdx \qquad (44)$$

the quark model predicts the value 0.278 while the experimental data give 0.125. We conclude that only 50% of the linear momentum of the nucleon are carried by quarks. Obviously, the remaining half must be carried by gluons.

In a similar way as in eq. (42) the polarized structure functions are related to distribution functions for quarks with spin parallel (f) or antiparallel (↓) to the total spin of the nucleon. Neglecting the small longitudinal contributions, we have for the transverse-transverse structure function

$$G_1 \longrightarrow^{DIS} \frac{1}{M^2\omega_L} g_1(x), \qquad (45)$$

and

$$g_1(x) = \frac{1}{2}\sum_q e_q^2 \left(f_q^{\uparrow}(x) - f_q^{\downarrow}(x)\right). \qquad (46)$$

With the definition

$$\Delta_q = \int_0^1 \left(f_q^{\uparrow}(x) - f_q^{\downarrow}(x)\right) dx, \qquad (47)$$

the total probability to find the quarks with spin in the direction of the nucleon's spin should be related to

$$\Gamma_1 = \int_0^1 g_1(x)dx = \\ = \frac{1}{2}\left(\frac{4}{9}\Delta u + \frac{1}{9}\Delta d + \frac{1}{9}\Delta s\right)\left(1 - \frac{\alpha_s(Q^2)}{\pi}\right) \qquad (48)$$

The last factor on the rhs is the lowest order radiative correction for QCD. It leads to a weak dependence of $\Gamma_1$ on the momentum transfer $Q^2$.

According to the 'Ellis-Jaffe sum rule'[38] the integrals should have the following values for proton ($\Gamma_1^p$) and neutron ($\Gamma_1^n$), respectively:

$$\Gamma_1^p = \frac{g_A}{12}\left(1 + \frac{5}{3}\frac{3r-1}{r+1}\right)\left(1 - \frac{\alpha_s}{\pi}\right) \qquad (49)$$

$$\Gamma_1^n = \frac{g_A}{12}\left(-1 + \frac{5}{3}\frac{3r-1}{r+1}\right)\left(1 - \frac{\alpha_s}{\pi}\right), \qquad (50)$$

where r = $F/D \approx 2/3$ from $SU(3)$ of the flavours $u$, d and $s$. The model-dependent quantity r cancels in the isovector combination

$$\Gamma_1^p - \Gamma_1^n = \frac{g_A}{6}\left(1 - \frac{\alpha_s}{\pi} + [\alpha_s^2]\right), \qquad (51)$$

the so-called 'Bjorken sum rule'[39]. The appearance of the axial coupling constant $g_A$ is due to the fact that the combination $\vec{J}^+ \times \vec{J}$ leading to $G_1$ is an axial vector, hence related to the axial current of the nucleon. As a result, eq. (51) is a direct consequence of QCD.

The 'spin crisis' was generated in 1988 by the EMC group[40] who derived

$$\Gamma_1^p(exp) = 0.116 \pm 0.012 \pm 0.026 \qquad (52)$$

from their data, inciuding the statistical and systematical errors. It differed substantially from the value predicted by eq. **(49)** with r taken from $SU(3)$ considerations,

$$\Gamma_1^p(theory) = 0.191 \pm 0.002. \qquad (53)$$

The results of this experiment and of the theoretical expectation are shown in Fig. 12.

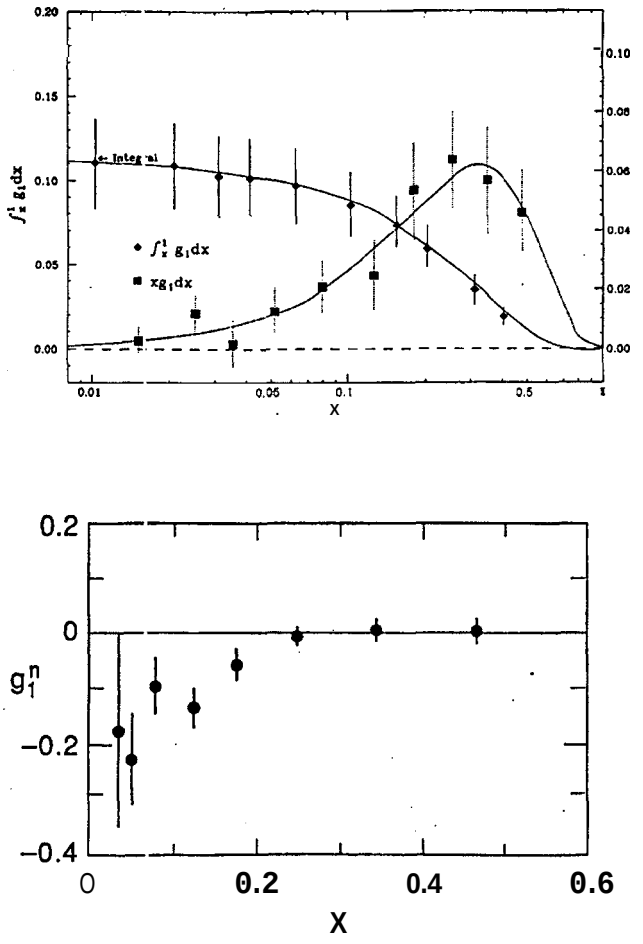


Figure 12: Upper part: The EMC spin structure function, $xg_1^p(x)$, for the proton and the corresponding integral $\Gamma_1(x)$, see eq. (48). [40] Lower part: The spin structure function for the neutron $g_1^n(x)$, extracted from the SLAC data. [43].

In conjuriction with other DIS data, this blatant discrepancy leads to the conclusion that the spin contribution of the valence and sea quarks should cancel, and that the total spin of the nucleon should be given by gluons and, possibly, quark angular momentum (D-state, bag deformation). As has been pointed out by Close[41] the discrepancy is actually considerably reduced. A reevaluation of the data led to a slight increase of the integral,

$$\Gamma_1^p\,(exp) = 0.126\text{-f}\ 0.011 \pm 0.014, \qquad (54)$$

and a new analysis of the model-dependent parameter r lowers the theoretical value,

$$\Gamma_1^p\,(\text{theory}) = 0.175 \pm 0.007. \qquad (55)$$

The two values are still at variance, but at a much reduced level. As a consequence the results of Fig. 12 will have to be 'renormalized'.

The discussion about the spin crisis triggered considerable experimental activities to measure the structure function of the neutron, in particular to test the Bjorken sum rule, eq. (51). The question has been addressed in two recent publications of the SMC group at *CERN*[42] and the E142 collaboration at *SLAC*[43]. The SMC group measured the scattering of polarized electrons off a polarized deuterium target in the kinematical range $0.006 < x < 0.6$ and $1\text{GeV}^2 < Q^2 < 30\text{GeV}^2$. Combining their data for $\Gamma_1^d \approx \Gamma_1^p + \Gamma_1^n$ with the previously measured value for $\Gamma_1^p$, they obtained

$$\Gamma_1^p - \Gamma_1^n = 0.20 \pm 0.05 \pm 0.04 \qquad (56)$$

in good agreement with the Bjorken sum rule, $0.191 \pm 0.002$, as derived from eq. (51). The SLAC group, on the other side, used polarized $^3He$ as a target to derive a first result for the polarized neutron (the two protons in $^3He$ cancel to lowest order !),

$$\Gamma_1^n = -0.022 \pm 0.011. \qquad (57)$$

This value agrees with the naive quark model (eq. (50) evaluated with $r = 2/3$). However, the combination with the existing proton data leads to a considerable contradiction with the Bjorken sum rule, i.e. with QCD. Since the SLAC data have been taken at smaller momentum transfer, $1\text{GeV}^2 < Q^2 < 6\text{GeV}^2$, and for a smaller range of the Bjorken variable, $0.03 < x < 0.06$, a direct comparison of the data and the combination of different data sets should be performed with great care. Using reasonable corrections for the $Q^2$ evolution, Close[41] has reanalyzed the existing experimental information. As has been shown in table 2, the combination of the EMC and SMC data disagrees with the quark model but fulfils the Bjorken sum rule, while the combination of the SLAC results with either the EMC or the SMC data violates the Bjorken sum rule. The table shows that it may be too early to draw definite conclusions about the carriers of the nucleon's spin.

Of course, the naive quark model predicts that the spin should be carried by the quarks only. The contribution of the u, d and $s$ quarks should add to an

Table 2: The spin integrals for the proton ($\Gamma_1^p$) and the neutron ($\Gamma_1^n$) obtained for combinations of the EMC[40], SMC[42] and SLAC[43] data, in comparison with the theoretical predictions according to Close[41]. See eqs. (48-51) and text.

| | $\Gamma_1^p$ | $\Gamma_1^n$ | $\Gamma + \Gamma$ | $\Gamma_1^p - \Gamma_1^n$ |
|---|---|---|---|---|
| theory | 0.173 | -0.019 | 0.154 | 0.192 |
| EMC/SMC | 0.13 ± 0.2 | -0.08± 0.06 | | 0.21 ± 0.06 |
| SLAC/EMC | | -0.02 ± 0.01 | 0.10 ± 0.03 | 0.15 ± 0.02 |
| SLAC/SMC | 0.07 ± 0.06 | | 0.05 ± 0.05 | 0.09 ± 0.08 |

expectation value of $\frac{1}{2}$ for the total spin of the proton,

$$\sum_q \langle S_z \rangle_q = \frac{1}{2} \sum_q \Delta q = 0.5, \qquad (58)$$

with $\Delta u = \frac{4}{3}$, $\mathrm{A}d = -\frac{1}{3}$ and $\mathrm{A}s = 0$ in the constituent quark model. It is well known, however, that this model gives a wrong value for the axial coupling constant,

$$g_A = \frac{5}{3}(\Delta u + \mathrm{A}d) = \frac{5}{3} \neq 1.26 \quad \text{(experiment!)}. \qquad (59)$$

Furthermore, the $SU(3)$ symmetry is broken and tlie nucleon acquires a small contribution of s−quarks, $\mathrm{A}s \approx -0.15$. In conclusion we may expect

$$\sum_q \langle S_z \rangle_q = \frac{1}{2}(\Delta u + \mathrm{A}d + \mathrm{A}s)$$
$$= \frac{3}{5} g_A \left(1 - 4\frac{2-3r}{1+r}\right) \approx 0.29, \qquad (60)$$

considerably below tlie "naive" prediction of the quark model, eq. (58).

As has been stated before, also the "experimental data" have moved towards a compromise with theory. The result has been shown in table 3 indicating the most likely answer at this time: About 50 % of the spin of the proton is directly carried by the quarks, the other half has to be carried by the gluons. This is essentially the same answer as in the case of the linear momentum of the nucleon.

## VI. Summary and conclusion

Investigations with electromagnetic interactions have contributed substantially to a better understanding of the structure of the nucleon. We have concentrated in this review on the two limiting cases, elastic scattering, i.e. a completely coherent reaction with regard to the partons of the nucleon, and deep inelastic scattering (DIS), i.e. the idealized case of incoherent reactions with the individual partons. These carriers of charge and magnetization are the quarks, existing in the form of valence and sea quarks. Their motion is governed by tlie laws of QCD, and the general structure of the electroweak interaction with quarks and nucleons is well understood. However, we cannot yet calculate the wave functions of the quarks, and therefore the matrix elements of the vector and axial vector currents involved have to be parametrized in terms of nucleon form factors and quark distribution functions. The goal of the experiments is to measure these structure functions over a wide kinematical range in order to test the theoretical predictions about the structure of hadrons.

A new generation of high-energy, high-intensity c. w. accelerators has opened exciting perspectives for a series of new experiments involving polarization degrees of freedom. In the area of elastic electron scattering we expect a model-independent separation of the electric and magnetic form factors of proton and neutron over a wide range of momentum transfer. New information is particularly important in the case of the neutron whose charge distribution may serve as a very critical test of models of the confinement phase. Parity-violating electron scattering allows to measure asymmetries due to the interferences between electromagnetism and weak interaction. These experiments are expected to provide a direct measurement of the strangeness content of the nucleon, i.e. the influence of the strange sea on charge and magnetization distributions. The strangeness content and the role of $s\bar{s}$ pairs has been a central point of uncertainty in many analyses of hadronic structure in the confinement phase (condensates, sigma term,

Table 3: The contribution of the quarks to the total angular momentum of tlie proton (in per cent).

| | u | d | s | valence | sea | total |
|---|---|---|---|---|---|---|
| naive CQM | 133 | -33 | - | 100 | - | 100 |
| refined *theory*[41] | | | | | | 58 |
| old analysis[23] | 78 | -48 | -20 | 107 | -97 | 10 |
| new analysis[41] | | | | | | 42 |

anomalies, spin crisis). The analysis of these experiment will also require better data for the neutron form factor.

New experiments are also necessary in the area of DIS. While the experiments agree that only half of tlie momentum of the nucleon is carried by the quarks, the situation is still quite open in the case of tlie spin. It is now realized that the 'spin crisis' might not be as dramatic as originally reported and that only about half of the spin might be 'missing', i.e. carried by gluons or by the orbital angular momentum of the quark-gluon system. The present experiments are somewhat contradictory among themselves. The essential problems remaining at tbis pcint are the deviations from scaling (dependente on monentum transfer, particularly for tlie data at low $Q^2$) and the question, how much of tlie overall strength is evolved into the polarized sea. One of the cleanest answers to the latter aspect is expected from a semi-inclusive experiment planned at HERA ('HERMES Collaboration'), a measurement of the $K^-(s\bar{u})$ production as function of the polarization of beam and target.

The advent of a new generation of accelerators and continuing progress in handling polarized beams and targets will provide a chance to ask questions at an unprecedented level of accuracy, and tlie answer to these questioris is expected to qualitatively improve our knowledge of the internal structure of hadrons in terms of quarks and gluons.

## References


1. D. Bailir. and A. Love, Introduction to gauge *field* theory, A.. Hilger, Bristol and Boston (1986).
2. I. J. R. Aitchison and A. J. G Hey, Gauge theories *in partic!e* physics, A. Hilger, Bristol (1984).
3. D. Drechsel and M. M. Giannini, Rep. Progr. Phys. 52, 1083 (1989).
4. T. W. Donnelly and A. S. Raskin, Ann. Phys. 169, 247 (1986).
5. P. E. Bosted et al., Phys. Rev. Lett. 68, 3481 (1992).
6. S. Galster et al., Nucl. Phys. B32, 221 (1971).
7. S. Platclikov et al., Nucl. Phys. **508A**, 343c (1990).
8. S. J. Brodsky and G. R. Farrar, Phys. Rev. Lett. 31, 1153 (1973).
9. P. Kroll, M. Schurmann and W. Schweiger, Z. Phys. **A338**, 339 (1991).
10. N. Isgur and G. Karl, Phys. Rev. **D18**, 4187 (1978) and **D19**, 2653 (1979).
11. M. M. Giannini, Rep. Progr. Phys. 54, 453 (1991).
12. A. W. Thomas, S. Théberge and G. A. Miller, Phys. Rev. D24, 216 (1981) 216; A. W. Thomas, Adv. in Nucl. Phys. 13, 1 (1984).
13. K. Bermuth et al., Phys. Rev. D37, 89 (1988).
14. A. Z. Gorski, G. Grummer and K. Goeke, Phys. Lett. B (1991).
15. U. G. Meissner, N. Kaiser and W. Weise, Nucl. Phys. **A466**, 685 (1987).
16. G. Hohler et al., Nucl. Phys. **B114**, 505 (1976).
17. H. Arenhovel, Phys. Lett. **B199**, 13 (1987).
18. C. E. Jones-Woodward et al., Phys. Rev. C44, R 571 (1991).
19. A. K. Thompson et al., Phys. Rev. Eett. **68**, 2901 (1992).
20. Th. Walcher, Proc. of Few-Body XIV, Amsterdam 1993.
21. CEBAF PR-93-038, R. Madey et al. (1993).
22. CEBAF PR-93-026, D. Day et al. (1993).
23. R. Decker, M. Nowakowski and U. Wiedner, Fort.

Phys. 41, 87 (1993).
24. T. W. Donnelly et al., Nucl. Phys. **A503**, 589 (1989).
25. R. L. Jaffe, Phys. Lett. **B229**, 275 (1989).
26. C. Y. Prescott et al., Phys. Lett. **77B**, 1 (1978).
27. W. Heil et al., Nucl. Phys. **B327**, 1 (1989).
28. P. A. Souder et al., Phys. Rev. Lett. 65, 65 (1990).
29. D. H. Beck, Proc. of Workshop on Parity Violation in Electron Scattering, eds. E. J. Beise and R. D. McKeown, World Scientific (Singapore).
30. D. von Harrach et al., A4 collaboration, Mainz proposal (1992).
31. CEBAF PR-91-017, D. Beck et al. (1991, revised 1992).
32. CEBAF PR-91-010, R. Souder et al. (1991).
33. CEBAF PR-91-004, E. Beise et al. (1991).
34. Park, Schechter, Weigel, Phys. Rev. D43, 869 (1991).
35. J. D. Bjorken, Phys. Rev. 179, 1547 (1969).
36. S. R. Mishra and F. Sciulli, Ann. Rev. Nucl. Part. Sci. **39,** 259 (1989).
37. V. W. Hughes, Ann. Rev. Nucl. Part. Sci. 33, 611 (1983).
38. J. Ellis, R. L. Jaffe, Phys. Rev. **D9**, 1444 (1974), **D10**, 1669 (1974).
39. J. D. Bjorken, Phys. Rev. 148, 1467 (1966).
40. J. Ashman et al., Phys. Lett. **B206**, 364 (1988) and Nucl. Phys. **B328**, 1 (1989).
41. F. Close, Proc. $6^{th}$ Workshop on Persp. in Nucl. Phys. at Intermediate Energies, Trieste (1993).
42. B. Adeva et al., Phys. Lett. **B302**, 553 (1993).
43. P. Anthony et al., Phys. Rev. Lett. 71, 959 (1993).